Highlights

- Microcosm experiments to investigate soils amended with softwood-derived biochars
- Volatilization of NH_3 was significantly impeded in alkaline sandy soils
- Retention of NO_3 by the biochar was not evident
- Mobilization of trace elements upon water inundation was significantly reduced
- Biochar produced at a higher pyrolysis temperature had better effects

Effects of Softwood Biochar on the Status of Nitrogen Species and Elements of Potential Toxicity in Soils

Natalie Heaney, Mufidat Mamman, Hajara Tahir, Ahmed Al-Gharib and Chuxia Lin*

School of Environment and Life Science, University of Salford, Greater Manchester M5 4WT United Kingdom

*Corresponding Author: Email: C.Lin@salford.ac.uk

ABSTRACT

The effects of softwood-derived biochar materials on the chemical behaviour of environmental contaminants in soils were examined in two microcosm scenarios. Addition of the biochar materials into an alkaline sandy soil significantly reduced NH_3 volatilization and made it available for conversion into NO_3^- via nitrification. This process could be enhanced by an increased application rate of biochar produced at a higher pyrolysis temperature. Under the alkaline conditions encountered in the experiment, the biochar surfaces tended to be negatively charged which disfavours the adsorption of NO_3^-. Therefore, in a fully open system, the addition of biochar materials was likely to contribute to nitrate leaching from the fertilized alkaline sandy soil. The effects of the biochar materials on the immobilization of Fe^{2+} generated via anaerobic iron reduction in the inundated contaminated soil were not observed, except for the treatment with a higher dose of biochar material produced under pyrolysis temperature at 700^{o}C after the 240th h of incubation. Arsenic showed similar behaviour to Fe. Zn tended to have a higher affinity to the biochar, as compared to Mn. Immobilization of Pb occurred regardless of whether or not the biochar is present.

Key words: Biochar, soil, nitrogen, heavy metals, environmental remediation

1 Introduction

Biochar produced from pyrolysis of biomass is thought to be an ideal product for improvement of soil fertility, remediation of contaminated soils, and long-term storage of carbon (Beesley et al., 2011; Jeffery et al., 2011; Tang et al., 2013; Ahmad et al., 2014). In recent years, there have been increasing investigations into the effects of biochar on removing a range of environmental pollutants from water and soil environments (Beesley et al., 2010; Ahmad et al., 2016). So far, the available publications reveal mixed results, showing that biochar may enhance, inhibit or have no effects on a pollutant of concern, depending on the biochar type used and the environmental conditions under investigation (Ahmad et al., 2014).

Biochar can be produced using a wide variety of organic feedstock such as woods, grasses, manures and organic waste materials (Mukome et al., 2013). The nature of feedstock, together with the operational conditions for pyrolysis, could markedly affect the physical and chemical characteristics of biochar (Aller, 2016). This explains the inconsistent observations on biochar-driven pollutant immobilization by different researchers who used different types of biochar in their experiments. To date, despite increased available information on biochar, there has still been insufficient understanding to allow generalization of biochar functions in terms of their uses for environmental remediation. This demands substantial further study to cover a wider range of biochar types in various environmental scenarios.

In this study, biochar materials produced from softwood pellets at two different pyrolysis temperatures were selected to observe their effects in two scenarios: (a) chemical behaviour of added ammonium in sandy soil and (b) immobilization of arsenic and heavy metals in a contaminated soil under water inundation conditions. The abundant organic waste from wood processing is an important source of biomass for biochar production (Komkiene and

Baltrenaite, 2016). Wood-derived biochar materials also tend to contain less polycyclic aromatic hydrocarbons (PAHs), as compared to those produced from other biomass types (Buss et al., 2016). This makes wood-originated biochars more attractive for being used as a remediating agent for soil contamination.

Ammonium-based chemical fertilizers are widely used for agricultural production (Fowler et al., 2013). Upon application, ammonium may be lost from soils through volatilization of ammonia if the soil pH is sufficiently high (Cameron et al., 2013). Microbially-mediated oxidation of ammonium (nitrification) can lead to the emission of gaseous nitrogen species and formation of nitrate (NO_3^-). Nitrate has a weak affinity to soil colloids and therefore is easier to mobilize under most soil conditions (Barber, 1995; Dickinson and Murphy, 2008). Under anaerobic conditions, nitrate can be reduced to form nitrogen gas (denitrification), leading to further nitrogen loss from soils (Cameron et al., 2013). Alkaline sandy soils are particularly prone to loss of nitrogen due to their weak capacity to adsorb ammonium and high water permeability. Furthermore, alkaline soils have favourable pH conditions for ammonia volatilization (Schomberg et al., 2012). The better availability of free ammonium in sandy soils owing to weak ammonium adsorption may also enhance nitrification. A few studies have shown that biochar can enhance retention of nitrogen in coarse-textured soils. Yao et al. (2012) reported that application of Brazilian pepperwood and peanut hull biochar (pyrolyzed at 600^{o}C) reduced NO_3^- leaching by 34.3% and 34%, respectively. Jarrah wood biochar (pyrolyzed at 600^{o}C) has also been found to significantly reduce NO_3^- leaching from sandy soil by 25% (Dempster et al., 2012). It is widely believed that a pyrolysis temperature >600^{o}C tends to be more favourable for producing biochar with a greater capacity to retain NO_3^- (Hale et al., 2013; Hollister et al., 2013). Higher production temperatures are known to increase biochar surface areas and possibly the number of adsorption sites for nitrogen

species. This could also increase water holding capacity of soils and consequently reduce the degree of nitrogen leaching (Uzoma et al., 2011). However, Gai et al. (2014) found that the biochar produced at 600-700^{o}C using different feedstock in an aqueous batch study was ineffective for NO_3^- retention. Therefore, the efficacy of biochar to retain N species could also be markedly affected by the inherent physiochemical properties of individual biochar and the environmental conditions into which the biochar is applied.

In a previous investigation, it was found that arsenic and heavy metals present in contaminated soils could be released under water inundation conditions in the presence of grass clippings (Mukwaturi & Lin, 2015). This represents a potential threat to the environment surrounding the contaminated sites. To minimize the environmental risk from contaminated sites, appropriate remediation measures need to be taken. It has been demonstrated that biochar has the capacity to immobilize a range of environmental pollutants (Park et al., 2016). It is therefore considered that biochar may have the potential for being used as a soil conditioner for minimizing the mobilization of elements of potential toxicity from the contaminated soils during flood inundation, which is worthy of investigation.

2 Materials and Methods

2.1 The biochar materials used in the experiments

Two softwood-derived biochar materials with pyrolysis temperatures at 550^{o}C and 700^{o}C (labelled as SWP550 and SWP700, respectively) were used for the microcosm experiments in this study. These biochar materials were purchased from the United Kingdom Biochar Research Centre (UKBRC). The major physical and chemical characteristics, as provided by the manufacturer, are given in Supplementary Table S1. Prior to their uses in the

experiments, the biochar samples were oven-dried at 40^{o}C for 48 hours and then ground using a mortar and a pestle to pass through a 2 mm sieve with a portion of the sample being further ground and passed through a 63 μm sieve for FTIR analysis.

2.2 The sandy soil used in Experiment 1

The sandy soil sample was collected from a construction site at the University of Salford, Manchester. After collection, the soil was oven-dried at 40^{o}C for 48 hours, gently crushed using a mortar and a pestle, and passed through a 2 mm sieve. All gravels with a particle diameter >2 mm were discarded. Some of the major physical and chemical characteristics are provided in Supplementary Table S1.

2.3 The contaminated soil used in Experiment 2

The contaminated soil sample was collected from a closed landfill site in the Greater Manchester region, United Kingdom. After collection, the soil was oven-dried at 40^{o}C for 48 hours, gently crushed using a mortar and a pestle to pass through a 2 mm sieve. All gravels with a particle diameter >2 mm were discarded. Some major physical and chemical characteristics are provided in Supplementary Table S1.

2.4 Experiment 1: Nitrogen in sandy soil

Plastic bottles (125 mL) were used as batch reactors. For each biochar type, one control and two treatments were used (see Supplementary Table S2). Appropriate amounts of biochar, sand and NH_4Cl were placed in each bottle and thoroughly mixed using a glass rod, followed by adding 10 mL of ultrapure water. The reactors were then allowed to stand for 24 h. At the end of the experiment, 100 mL of ultrapure water was added into each bottle and shaken for 1

h on a rotary shaker. After shaking, 15 mL of the supernatants were removed for measurement of water-soluble ammonium and nitrate. The supernatant was then decanted by passing it through a filter paper (Whatman 40). All residues retained on the filter paper were put back into each bottle for further extraction by a KCl solution. 100 mL of 1M KCl solution was added into each bottle and shaken again on a rotary shaker for 1 h. 15 mL of supernatant was then taken for measurement of the KCl-extractable ammonium and nitrate. All the water and KCl extracts taken for measurements of different nitrogen species were frozen before analysis by ion chromatography.

2.5 Experiment 2: Arsenic and heavy metals in contaminated soil

A microcosm experiment was conducted to observe the temporal variation in several parameters following water inundation. Plastic bottles (500 mL) were used as batch reactors. Prior to the experiment, the bottles were washed with nitric acid and rinsed with deionised water, followed by drying. One control (added grass clippings but no added biochar, labelled as C) and two biochar treatments were set for each biochar type. Details on experimental set-up are shown in Supplementary Table S3. In each reactor, 50 g of soil was placed into the bottle. For C, Treatment 1 and Treatment 2, 5 g of fresh grass clippings (chopped to 1 cm in length) was added into the bottle. For Treatment 1 and Treatment 2, 0.5 or 2 g of biochar was added, respectively. The contents of each bottle were thoroughly mixed by a glass rod and then 200 mL of ultrapure water (18.2 MΩ cm) was poured into the bottle to create water inundation conditions. The bottles were capped and agitated by hand for 1 min and then allowed for standing on the laboratory bench. The experiment was run for 15 days. During the incubation experiment, monitoring of various parameters were made from the 1st h of the experiment. Subsequent sampling was performed at the 24th, 48th, 120th, 240th and 360th h

following the commencement of the experiment. pH, electrical conductivity (EC) and dissolved oxygen (DO) were measured in-situ using a pH meter (Jenway-3510), EC meter (Mettler Toledo) and DO meter (Oxyguard Handy MK1 DO), respectively. After this, 10 mL of the overlying water later was taken for measurements of different trace elements. The samples were passed through a 0.22 µm syringe filter and acidified by adding 2 drops of nitric acid. The solution was then stored in the fridge at 4^{o}C before analysis.

2.6 Analytical Methods

The surface morphology and structure of the biochar samples were observed using a Philips XL30 SFEG scanning electron microscope (SEM). The micrographs were acquired using an accelerating voltage of 7KV with a spot size of 3 and secondary electron detection (SE). Surface functionality of the biochar samples was analysed by Fourier transform infrared spectroscopy (FTIR) (Thermo Fischer Nicolet IS10) with a spectral resolution of 16 cm^{-1}. Spectrograph v1.0.5 software was used to assist in the interpretation of the results. Pre-analysis was done using 16 co-added scans. However, a better signal-to-noise ratio was found at 100 scans, which was then used for obtaining the final results.

The pH, EC and DO in solution samples were measured by a Jenway-3510 pH meter, a Mettler Toledo EC meter and an Oxyguard Handy MK1 DO meter, respectively. Numerous trace elements were measured by inductively coupled plasma optical emission spectrometry (Varian 720ES ICP-OES). The concentrations of NH_4^+ and NO_3^- in the aqueous samples were determined by ion chromatography (DIONEX ICS-1000). For the determination of NH_4^+, an IonPac® CS12A analytical column (4 mm×250 mm), IonPac® CG12A guard column (4 mm×50 mm), and RFIC cation self-regenerating suppressor 300 *(*4 mm) were used. 20 mM methanesulphonic acid was used as the mobile phase. For the measurements of NO_3^-, an

IonPac® AS14 anion analytical column (4 mm×250 mm), IonPac® AG14 guard column (4 mm×50 mm), and ULTRA Ⅱ *anion* self-regenerating suppressor (4 mm) were used. A mixed 0.8 mM sodium carbonate (Na_2CO_3) and 1 mM sodium bicarbonate solution was used as the mobile phase. The flow rate was set at 1.0 mL/min with 20 μL injection volume.

2.7 QA/QC and statistical analysis

All experiments were performed in triplicate. All chemical reagents used in the experiments were of analytical reagent grade. Ultrapure water (18.2 MΩ/cm) was used throughout the entire course of all the experiments. The data for the different treatments and the different sampling times for each treatment were separately analysed using one-way ANOVA with Duncan's post-hoc test to determine statistical significance (Assad et al., 2014). All data are displayed as the mean ± standard error of the mean.

Repeatability analysis for experiment 1 shows mean relative standard deviation (RSD) was 0.27% for water extractable NH_4^+, 0.02% for water extractable NO_3^- and 0.31% for KCl extractable NH_4^+. For experiment 2, RSD values were 0.06% for pH, 0.59% for EC, 1.21% for DO, 1.34 for Fe, 1.25% for Mn, 0.39% for As, 0.69% for Zn and 0.41% for Pb, respectively.

3 Results

3.1 SEM Results

The micrographs of SWP550 and SWP700 are shown in Supplementary Fig. S1. There was a marked difference in capillary structure between the two biochar materials. SWP550 showed a rough surface with folded structures, thicker pore walls and a flaky surface whereas

SWP700 showed a more regular honeycomb structure, which originated from the original tubular structure of plant biomass (Nartey & Zhao, 2014). SWP700 had thinner walls separating macropores. The formation of mesopores (and potentially micropores) could be seen within certain macropores, and this made SWP700 have higher surface area. The surface of SWP700 was laminated and glossy, as compared to that of SWP550. These results were in good agreement with what was found by Gai et al. (2014).

3.2 FTIR Results

The FTIR spectra for the two biochar materials can be seen in Fig. 1. No significant peak was detected in the region beyond 2000 cm^{-1}. SWP700 showed an increased baseline shift, as compared to SWP550. Peaks between 640-860 cm^{-1} can be assigned to C-H out of plane vibrations (Mukome et al., 2013). Two concurrent peaks occurred at 1118 cm^{-1} and 1182 cm^{-1}, that can be assigned to C-C and C-O stretching, respectively (Zeng et al., 2013). A further 2 peaks can be seen at 1437 cm^{-1} and 1490 cm^{-1}, which are likely to be linked to CH_2 groups. The peak near 1600 cm^{-1} may be assigned to C=C bonds.

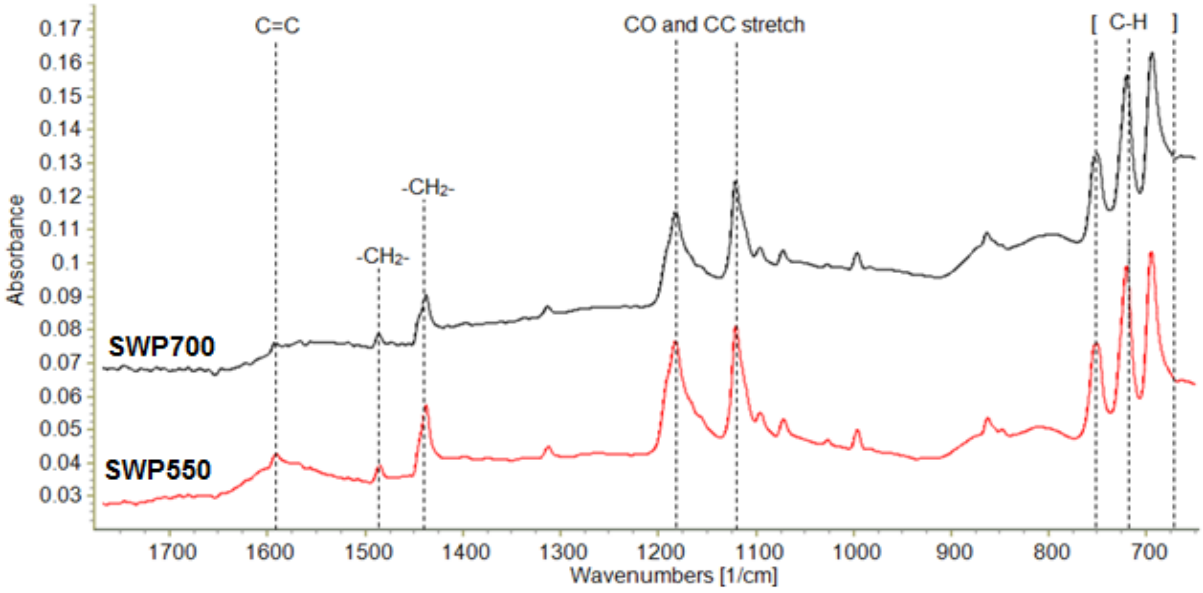

Figure 1 - The FTIR spectra for SWP550 and SWP700

209

210 **3.3 Experiment 1: Nitrogen in sandy soil**

211 At the end of the incubation experiment, the concentration of either NH_4^+ or NO_3^- in the
212 water extract showed the following trend, 1 g > 0.5 g > Control (significant at $P<0.05$) for
213 both SWP550 or SWP700. In the control, the amount of NH_4^+ is extremely low (see Fig. 2).
214 No statistically significant difference in water-extractable NH_4^+ or NO_3^- was observed
215 between the lower dose of SWP550 and SWP700. However, when a higher dose (1 g) of each
216 biochar was applied, a statistically significant increase ($P<0.05$) could be observed,
217 suggesting pyrolysis temperature significantly affects the water-extractable N species at
218 higher doses. No KCl-extractable NO_3^- was detected for the control and any treatments.
219 NH_4^+ was significantly different between the control and the treatments, showing the

following increasing trend: Control < 0.5 g SWP550 < 0.5 g SWP700 < 1 g SWP550 < 1 g SWP700 (significant at $P<0.05$, except for 1 g SWP700 vs 1 g SWP550 treatments) (Fig. 2).

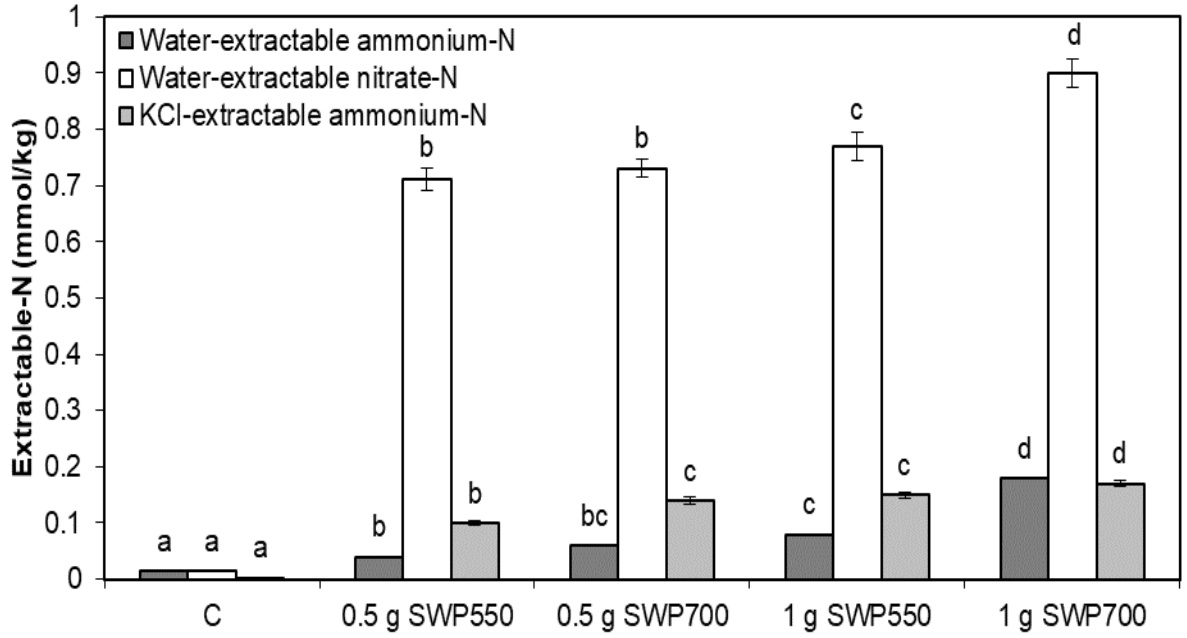

Figure 2 Concentration of water-extractable ammonium-N, water-extractable nitrate-N and KCl-extractable ammonium-N in the control and various treatments. All values are presented as the mean ± standard error (n=3), and bars with different letters for each parameter indicate a significant difference ($P < 0.05$) according to Duncan's post hoc test.

3.4 Experiment 2: Arsenic and heavy metals in the contaminated soil

3.4.1 Changes in pH, EC and DO during the period of incubation experiment

At the 1st h following the commencement of the incubation, the pH in the overlying water layer ranged from 5.44 to 5.57 for the control and treatments. The pH in the control was generally higher than that in the treatments in the early stages of the experiment and was significantly higher by the 24th h. On any subsequent sampling occasions, no significant difference in pH was observed. There was a clear trend showing that EC increased over time.

Treatments with the lower dose of either SWP550 or SWP700 tended to have low electrical conductivity compared to SWP700 containing treatments and the control, though a significant difference was not always observed. DO at the 1st h ranged from 6.1 to 8.5 mg/L but sharply dropped at the 24th h and then slowly decreased until the end of the experiment (Table 1). Statistical significance was not achieved between control and any of the biochar-containing treatments, at any time interval.

Table 1 Mean pH, electrical conductivity (EC) and dissolved oxygen (DO) in the water layer overlying the soil at different sampling times for the control and various treatments during the period of the incubation experiment

Parameter	Treatment	1 h	2 4 h	48 h	120 h	240 h	360 h
pH	Control	5.57±0.03Aba	5.79±0.02Aa	4.74±0.27Da	5.05±0.04CDa	5.05±0.04CDa	5.22±0.04BCa
	0.5 g SWP550	5.49±0.07Aa	5.70±0.01Ab	5.25±0.01Aa	5.24±0.24Aa	5.24±0.24Aa	5.12±0.04Aa
	0.5 g SWP700	5.45±0.08Ba	5.69±0.02Ab	5.02±0.06Ca	5.03±0.03Ca	5.03±0.03Ca	5.14±0.07Ca
	2 g SWP550	5.44±0.05Aba	5.69±0.02Ab	5.23±0.11BCa	5.39±0.13ACa	5.39±0.13ACa	5.10±0.03Ca
	2 g SWP700	5.48±0.05Ba	5.73±0.02Ab	5.06±0.06Ca	5.04±0.08Ca	5.04±0.08Ca	5.16±0.06Ca
EC (dS/cm)	Control	221±21.5Ea	346±36.9Da	532±25.7Ca	738±32.4Ba	800±50.2Ba	1026±14.9Aa
	0.5 g SWP550	94.0±24.5Db	214±20.9Dbc	441±110Ca	612±91.0Ca	811±44.3Ba	1077±38.5Aa
	0.5 g SWP700	252±47.19Ea	307±39.0Ea	494±64.7Da	648±41.5Ca	792±44.7Ba	1040±36.2Aa
	2 g SWP550	124±4.68Eb	178±2.56Ec	310±14.1Da	466±27.5Ca	673±36.5Ba	951±68.2Aa
	2 g SWP700	249±32.3Ea	308±27.9Eab	501±49.0Da	662±51.7Ca	844±45.3Ba	1065±36.6Aa
DO (mg/L)	Control	6.63±0.58Aa	1.10±0.20BCa	1.07±0.15BCa	1.90±0.50Ba	0.67±0.07Ca	0.23±0.03Ca
	0.5 g SWP550	8.50±0.21Aa	3.77±1.52Ba	2.93±1.12BCa	0.60±0.10Ca	0.53±0.12Ca	0.53±0.09Ca
	0.5 g SWP700	7.97±1.18Aa	1.57±0.19Ba	1.33±0.35Ba	1.13±0.47Ba	0.63±0.12Ba	0.17±0.07Ba
	2 g SWP550	6.30±0.06Aa	3.27±0.62Ba	1.03±0.17Ca	2.03±1.23BCa	0.53±0.20Ca	0.33±0.09Ca
	2 g SWP700	6.10±1.86Aa	1.37±0.12Ba	1.13±0.83Ba	1.00±0.38Ba	0.73±0.12Ba	0.43±0.13Ba

All data are presented as mean ± standard error (n=3). Means with different uppercase letters in the same row (time) and lowercase letters in the same column (treatment) are significantly different at P <0.05 (Duncan's post hoc test).

3.4.2 Changes in the concentrations of arsenic and heavy metals during the period of incubation experiment

The temporal variation of different elements of potential toxicity for the control and various treatments during the period of incubation experiment are shown in Table 2. For Fe, there was a clear trend showing that the concentration increased over time for both the control and the treatments. It is interesting to note that Fe concentration was significantly higher in the control than in the treatments at the 1st h of the experiment. Yet the concentration of Fe tended to be lower in the 2 g SWP700 treatment, compared to the control and the other treatments after the 240th h of the experiment although statistically significant level was only achieved at the 360th h. The concentration of Mn generally showed a trend to increase over time. Like Fe, Mn concentration was significantly higher in the control than in the treatments at the 1st h of the experiment. Both SWP700 containing treatments tended to have a higher concentration of Mn after the 120th h, as compared to the control and other treatments with a statistically significant level was achieved. However, a significant difference between treatments was not maintained towards the end of the experiment. Arsenic also tended to increase at the later stage (started from somewhere between the 48th and 120th h). The 2 g SWP700 treatment had a significantly lower As concentration from the 240th h, as compared to the control and the other treatments. However, this was not observed at the 360th h. Zn exhibited a similar trend to Mn, showing a higher concentration ($P < 0.05$) in the 0.5 g SWP700 treatment than in the control and other treatments at the 120th h and 240th h. Also at the 240th h, Zn concentrations in the 2 g SWP700 treatment was significantly lower than that for the other treatments and control. By the 360th h, a significantly lower concentration of Zn was observed for the 2 g SWP700 treatment compared to that in the control and other treatments. There was no clear trend for temporal variation in Pb (Table 2), Cd, Cr and Cu (data not shown) though Cu concentration was significantly higher in

the control than in the treatments at the 1st h of the experiment, as observed for Fe, Mn and Zn (data not shown).

Table 2 Temporal variation in the concentrations in arsenic and heavy metals in the water layer overlying the soil during the period of incubation experiment

Element	Treatment	1 h	2 4 h	48 h	120 h	240 h	360 h
Fe (mg/L)	Control	1.59±0.49Ca	0.14±0.01Ca	2.21±0.26Ca	8.38±1.62Cc	30.22±2.34Ba	68.6±6.49Aa
	0.5 g SWP550	0.57±0.31Db	0.13±0.01Da	4.35±0.75CDa	9.20±0.51Cc	33.69±4.01Ba	64.9±1.12Aa
	0.5 g SWP700	0.14±0.01Db	0.13±0.00Da	3.76±1.75Da	14.46±1.66Cab	37.68±2.75Ba	66.3±3.25Aa
	2 g SWP550	0.16±0.02Cb	0.14±0.01Ca	3.79±0.54Ca	9.16±2.36Cbc	33.37±4.38Ba	64.9±5.08Aa
	2 g SWP700	0.11±0.01Db	0.14±0.00Da	2.23±1.58Da	15.25±1.57Ca	25.86±1.76Ba	36.5±6.69Ab
Mn (mg/L)	Control	1.16±0.48Ca	0.03±0.00Ca	2.38±0.08Ca	7.17±0.79Cb	19.14±1.91Ba	39.6±5.22Aa
	0.5 g SWP550	0.24±0.16Eb	0.03±0.00Ea	4.07±0.43Da	8.85±0.30Cab	21.20±1.87Ba	38.2±2.26Aa
	0.5 g SWP700	0.03±0.00Db	0.03±0.00Da	3.53±1.03Da	11.20±0.97Ca	26.61±1.71Ba	43.4±2.99Aa
	2 g SWP550	0.04±0.01Eb	0.03±0.00Ea	4.16±0.40Da	9.08±0.92Cab	22.17±1.47Ba	40.0±0.40Aa
	2 g SWP700	0.03±0.00Eb	0.02±0.00Ea	3.15±1.30Da	10.93±1.16Ca	21.30±0.55Ba	32.1±0.91Ab
As (mg/L)	Control	0.09±0.01Ba	0.08±0.01Ba	0.08±0.02Ba	0.11±0.01ABc	0.16±0.01Ab	0.15±0.04Aa
	0.5 g SWP550	0.08±0.01CDa	0.06±0.00Da	0.12±0.01BCa	0.16±0.01Bab	0.21±0.01Aa	0.17±0.03Ba
	0.5 g SWP700	0.07±0.01Ba	0.07±0.00Ba	0.07±0.02Ba	0.17±0.00Aa	0.16±0.01Ab	0.17±0.02Aa
	2 g SWP550	0.08±0.01Ca	0.07±0.00Ca	0.10±0.01BCa	0.13±0.01ABbc	0.15±0.03Ab	0.15±0.01Aa
	2 g SWP700	0.07±0.01Aa	0.06±0.00Aa	0.06±0.03Aa	0.10±0.02Ac	0.10±0.00Ac	0.07±0.03Ab
Zn (mg/L)	Control	1.78±0.44ABa	0.27±0.02Da	0.41±0.02Da	0.81±0.06CDb	1.28±0.07BCb	1.89±0.06Aa
	0.5 g SWP550	0.66±0.23CDb	0.25±0.00Ea	0.60±0.04Da	0.95±0.02Cb	1.52±0.13Bab	2.00±0.03Aa
	0.5 g SWP700	0.29±0.01Cb	0.25±0.01Ca	0.55±0.17Ca	1.30±0.15Ba	1.83±0.17Aa	2.15±0.10Aa
	2 g SWP550	0.34±0.02DEb	0.26±0.01Ea	0.58±0.03Da	0.95±0.09Cb	1.49±0.15Bab	2.06±0.09Aa
	2 g SWP700	0.25±0.01Ab	0.25±0.00Aa	0.44±0.19Aa	0.67±0.06Ab	0.76±0.12Ac	0.38±0.18Ab
Pb (mg/L)	Control	0.09±0.01Ba	0.12±0.01Ba	0.08±0.01AB	0.14±0.00Ab	0.14±0.05Aa	0.07±0.03ABa
	0.5 g SWP550	0.11±0.00Aa	0.10±0.01Aa	0.09±0.01Aa	0.11±0.02Abc	0.17±0.04Aa	0.11±0.03Aa
	0.5 g SWP700	0.12±0.00Aa	0.11±0.00Aa	0.13±0.03Aa	0.22±0.05Aa	0.11±0.03Aa	0.11±0.03Aa
	2 g SWP550	0.11±0.01Aa	0.12±0.00Aa	0.09±0.03Aa	0.14±0.01Ab	0.15±0.01Aa	0.13±0.02Aa
	2 g SWP700	0.11±0.01Aa	0.11±0.01Aa	0.06±0.04Aa	0.04±0.01Ac	0.09±0.05Aa	0.10±0.06Aa

All data are presented as mean ± standard error (n=3). Means with different uppercase letters in the same row (time) and lowercase letters in the same column (treatment) are significantly different at P <0.05 (Duncan's post hoc test).

4 Discussion

4.1 Effects of biochar materials on nitrogen status

The extremely low concentration of both water-extractable and KCl-extractable ammonium and nitrate in the control suggest that most of the added ammonium was lost during the period of the experiment. The sandy soil had a pH of 9.59, which is favourable for NH_3 volatilization:

$NH_4^+{}_{(aq)} + OH^-{}_{(aq)} \rightarrow NH_{3(g)} + H_2O_{(l)}$ [1]

Addition of biochar materials significantly reduced the loss of nitrogen. From Table 3, it can be seen that only 1% of the added nitrogen was retained in the control while the nitrogen retention rate for sandy soil amended with 0.5 g SWP550, 0.5 g SWP700, 1 g SWP550 and 1 g SWP700 was 42, 46, 50 and 63%, respectively. Many authors suggested that retention of ammonium by biochar was mainly through cation exchange (*e.g.* Ding et al., 2010; Hou et al., 2016; Zhu et al., 2012). However, the exchangeable NH_4^+ fraction, as indicated by the KCl-extractable NH_4^+, only accounted for a very small proportion of the nitrogen in the investigated system. A larger proportion of NH_4^+ was in a water-extractable form. Ammonia gas can be physically adsorbed by organic adsorbents (Helminen et al., 2001; Van Humbeck et al., 2014). It is therefore likely that the ammonia gas produced in Equation 1 can be adsorbed by the biochar materials:

$[Biochar] + NH_{3(g)} \rightarrow [Biochar]\text{-}NH_3$ [2]

The biochar-adsorbed ammonia can be dissolved in water and become bioavailable (Taghizadeh-Toosi et al., 2012). Consequently, the temporary retention of ammonia gas by biochar significantly reduced the rate of the ammonia volatilization and made them available for conversion into NO_3^- via nitrification. This explains the presence of NO_3^- in the treatments where no nitrate was detected in the control.

Table 3 Mass balance of nitrogen in the experimental system

Parameter	Control	0.5 g SWP550	0.5 g SWP700	1 g SWP550	1 g SWP700
Amount of N added (mmol/kg)	2	2	2	2	2
Water-extractable NH_4-N (mmol/kg)	0.02	0.04	0.06	0.08	0.18
Water-extractable NO_3-N (mmol/kg)	0.00	0.71	0.73	0.77	0.90
KCl-extractable NH_4-N (mmol/kg)	0.00	0.10	0.14	0.15	0.17
Sum of retained N (mmol/kg)	0.03	0.85	0.92	1.01	1.25
Nitrogen retention rate (%)	1	42	46	50	63

The dose effect was clear with an increase in added biochar from 0.5 g to 1 g resulting in a decreased rate of gaseous N loss by 8% and 17% for the SWP550 treatment and SWP700 treatment, respectively. This suggests that the increased application of biochar can enhance the retention of N species in soil. For the biochar materials produced from the same feedstock, the pyrolysis temperature tended to make the biochar more favourable for nitrogen retention (relative to the gaseous loss of nitrogen). This can be attributed to the larger surface area (Supplementary Table S1) and the presence of certain functional groups, which enhanced the adsorption of NH_4^+ chemically and ammonia gas physically. Ammonium sorption via electrostatic attraction to negatively charged functional groups has been previously documented. Aromatic C-C, C-O, -CH_2- and CC could be involved in NH_4^+ sorption onto biochar (Cui et al., 2013; 2016; Takaya et al., 2016;). These functional groups were present in SWP550 and SWP700 to some degree (Fig. 1). However, since the H/C and O/C values of the biochar materials were relatively low, it is likely that there were only a limited number of these functional groups present on the surfaces of the biochar materials (Jassal et al., 2015). This explains the observed low exchangeable NH_4^+, even in the biochar-amended soils.

The current experiment was set as a partially open system that only allowed a loss of nitrogen in the system through emission of gaseous N. The NO_3^- formed in the treatments was almost entirely in water-soluble form since no KCl-extractable nitrate was detected. This can be attributed to the alkaline nature of both the soil and the biochar (Supplementary Table S1). Under such pH conditions, the biochar surfaces tend to be negatively charged, which disfavours the adsorption of NO_3^-. Therefore, in a fully open system, the addition of biochar materials was likely to contribute to nitrate leaching from the fertilized sandy soil. Work by others (e.g. Hale et al., 2013; Hollister et al., 2013) found that biochar produced at pyrolysis temperature <600^{o}C (irrespective of feedstock) were unable to retain NO_3^- and therefore could contribute to NO_3^- leaching. Gai et al. (2014) also found

that biochar produced at >600^{o}C of pyrolysis temperature could not absorb NO_3^-, resulting in the release of NO_3^- into aqueous systems.

4.2 Effects of biochar materials on arsenic and heavy metals under water inundation conditions

In consistence with the previous findings, DO in the overlying water layer rapidly dropped following water inundation of the soil in the presence of grass clippings as a result of consumption of water-borne oxygen by organic matter-decomposing microorganisms (Mukwaturi & Lin, 2015). The reducing conditions enhanced the anaerobic reduction of iron and manganese oxides, which led to the mobilization of trace elements bound to these compounds (Frohne et al., 2011; Mukwaturi & Lin, 2015). The insignificant increase in the concentration of solution-borne heavy metals and arsenic from the 1st h to the 24th h reflects that the release of heavy metals and arsenic, as driven by microbially mediated iron reduction require more time (> 24 h) to be initiated. The higher concentration of Fe in the control, relative to all the treatments, at the 1st h of the experiment, was probably due to the presence of soluble Fe^{3+} because the soil pH was acidic (Supplementary Table S1). Addition of biochar materials effectively removed the soluble Fe^{3+}, possibly via adsorption or acid neutralization. The effects of biochar materials on immobilization of Fe^{2+} generated via anaerobic iron reduction were not observed except with for the 2 g SWP700 treatment (Table 2). This indicates that the softwood biochar materials with pyrolysis temperature at 550^{o}C were not effective for immobilizing the mobilized Fe. While the softwood biochar materials with pyrolysis temperature at 700^{o}C may be effective, a dose of 0.5% was not sufficient to make any significant immobilization of the released Fe. Enhanced immobilization of the liberated Fe was observed after the 240th h of incubation although significant effect could only be attained at the 360th h (Table 2).

345 The higher concentration of Mn and Zn in the control, relative to all the treatments, at the 1st h of the
346 experiment was due to the same reason as for Fe. Both Mn and Zn are slightly soluble under
347 moderately acidic conditions (Reddy & DeLaune, 2008; Wiegand et al., 2009). Arsenic is an
348 oxyanion and its solubility is not directly pH dependent. This may be the reason why the same
349 phenomenon (higher concentration in the control at the 1st h of the experiment) was not observed for
350 As. The significantly (P <0.05) lower As in 2 g SWP700, as compared to the control and other
351 treatment from the 240th h, suggests that immobilization of As only took place when the biochar
352 produced at 700 ^{o}C was used at an application rate that was sufficiently high. This trend is similar to
353 Fe, indicating a link between Fe immobilization and As immobilization in the current reaction
354 system. Since arsenic was predominantly bound to iron oxyhydroxides in the contaminated soil used
355 in the experiment, the release of arsenic was closely associated with reductive dissolution of iron
356 oxyhydroxides mediated by iron-reducing microbes. Therefore, the concentration of solution-borne
357 As tends to be related to the solution-borne Fe^{2+} in the investigated system. The solubility of Pb is
358 very low even at moderately low pH, which explains that relatively higher Pb in the control was not
359 observed. The effect of biochar on Mn immobilization was not significant. However, immobilization
360 of the released Zn could be significantly enhanced even just after 220 h of incubation when 1% of
361 the SWP700 biochar was added into the system, suggesting that Zn had a higher affinity to the
362 biochar, as compared to Mn under the set experimental conditions in this study. This agrees well
363 with work by Hodgson et al. (2016) who showed that the grass-based biochar removed 93% of Zn
364 from contaminated mine waters, suggesting a high affinity of the biochar materials for Zn. However,
365 given that feedstock and pyrolysis temperature can markedly affect physiochemical characteristics
366 (Aller, 2016), the enhanced immobilization of trace elements by SWP700 may occur due to the
367 higher surface area and porosity of this biochar material (162 m^2/g), as compared to SWP550 (26.4
368 m^2/g). This is in contrast to what was observed by Park et al. (2015; 2016) who found that other

metals had a preferential affinity to biochar over Zn. Unlike Zn that can maintain certain solubility under circumneutral pH conditions (Wiegand et al., 2009), Pb is practically insoluble at pH >5 (Casas and Sordo, 2011). This explains the extremely low concentration of Pb in the solutions, as also observed in a previous experiment (Mukwaturi & Lin, 2015). Under such a circumstance, immobilization of Pb occurred regardless of whether or not the biochar is present.

5 Conclusion

Addition of the softwood-originated biochar materials significantly reduced NH_3 volatilization and made it available for conversion into NO_3^- via nitrification. This process could be enhanced by an increased application rate of biochar produced at higher pyrolysis temperature. Under the alkaline conditions encountered in the experiment, the biochar surfaces tend to be negatively charged which disfavours the adsorption of NO_3^-. Therefore, in a fully open system, the addition of biochar materials was likely to contribute to nitrate leaching from the fertilized alkaline sandy soil.

The effects of the softwood biochar materials on the immobilization of Fe^{2+} generated via anaerobic iron reduction in the inundated contaminated soil were not observed except for the treatment with a higher dose of biochar material produced under pyrolysis temperature at 700^{o}C after the 360th h of incubation. Arsenic showed similar behaviour to Fe. Zn tended to have a higher affinity to the biochar, as compared to Mn. Immobilization of Pb occurred regardless of whether or not the biochar is present. It is important to note that by the end of the incubation experiment (the 360th h), only the higher-dosed biochar (2 g SWP700) treatment revealed a statistically significant lower concentration (P<0.05) for the investigated elements of potential toxicity except for Pb, as compared to the control.

Acknowledgements

The authors would like to thank Dr D.P.T Smith for his assistance in sample analysis and Geoff Parr for carrying out SEM analysis. The biochar materials used in this study was purchased from the UKBRC at the University of Edinburgh.

References

Abdel-Fattah, T. M., Mahmoud, M. E., Ahmed, S. B., Huff, M. D., Lee, J. W., & Kumar, S. (2015). Biochar from woody biomass for removing metal contaminants and carbon sequestration. *Journal of Industrial and Engineering Chemistry, 22*, 103-109.

Ahmad, M., Ok, Y. S., Rajapaksha, A. U., Lim, J. E., Kim, B.-Y., Ahn, J.-H., Lee, S. S. (2016). Lead and copper immobilization in a shooting range soil using soybean stover- and pine needle-derived biochars: Chemical, microbial and spectroscopic assessments. *Journal of Hazardous Materials, 301*, 179-186.

Ahmad, M., Rajapaksha, A. U., Lim, J. E., Zhang, M., Bolan, N., Mohan, D., Ok, Y. S. (2014). Biochar as a sorbent for contaminant management in soil and water: a review. *Chemosphere, 99*, 19-33.

Aller, M. F. (2016). Biochar properties: Transport, fate and impact. *Critical Reviews in Environmental Science and Technology, 46*(14-15).

Assaad, H. I., Zhou, L., Carroll, R. J., & Wu, G. (2014). Rapid publication-ready MS-Word tables for one-way ANOVA. *SpringerPlus, 3*(1), 474.

Barber, S. A. (1995). *Soil nutrient bioavailability: a mechanistic approach*: John Wiley & Sons.

Beesley, L., Moreno-Jiménez, E., & Gomez-Eyles, J. L. (2010). Effects of biochar and greenwaste compost amendments on mobility, bioavailability and toxicity of inorganic and organic contaminants in a multi-element polluted soil. *Environmental pollution, 158*(6), 2282-2287.

Beesley, L., Moreno-Jiménez, E., Gomez-Eyles, J.L., Harris, E., Robinson, B., Sizmur, T. (2011). A review of biochars' potential role in the remediation, revegetation and restoration of contaminated soils, *Environmental pollution*, 159(12), 3269-3282.

Buss, W., Graham, M. C., MacKinnon, G., & Mašek, O. (2016). Strategies for producing biochars with minimum PAH contamination. *Journal of Analytical and Applied Pyrolysis, 119*, 24-30.

Cameron, K. C., Di, H. J., & Moir, J. L. (2013). Nitrogen losses from the soil/plant system: a review. *Annals of Applied Biology, 162*(2), 145-173. doi: 10.1111/aab.12014

Casas, J.S., Sordo J. (2011). *Lead: Chemistry, Analytical Aspects, Environmental Impact and Health Effects*. Elsevier, 366 pp.

Chen, X., Chen, G., Chen, L., Chen, Y., Lehmann, J., McBride, M. B., & Hay, A. G. (2011). Adsorption of copper and zinc by biochars produced from pyrolysis of hardwood and corn straw in aqueous solution. *Bioresource Technology, 102*(19), 8877-8884.

Cui, X., Hao, H., Zhang, C., He, Z., & Yang, X. (2016). Capacity and mechanisms of ammonium and cadmium sorption on different wetland-plant derived biochars. *Science of The Total Environment, 539*, 566-575.

Dempster, D. N., Jones, D. L., & Murphy, D. V. (2012). Clay and biochar amendments decreased inorganic but not dissolved organic nitrogen leaching in soil. *Soil Research, 50*(3), 216-221.

Dickinson, G., & Murphy, K. (2008). *Ecosystems: A Functional Approach*: Taylor & Francis.

Ding, Y., Liu, Y.-X., Wu, W.-X., Shi, D.-Z., Yang, M., & Zhong, Z.-K. (2010). Evaluation of biochar effects on nitrogen retention and leaching in multi-layered soil columns. *Water, Air, & Soil Pollution, 213*(1-4), 47-55.

Fowler, D., Coyle, M., Skiba, U., Sutton, M. A., Cape, J. N., Reis, S., . . . Voss, M. (2013). The global nitrogen cycle in the twenty-first century. *Philosophical Transactions of the Royal Society B: Biological Sciences, 368*(1621). doi: 10.1098/rstb.2013.0164

Frohne, T., Rinklebe, J., Diaz-Bone, R. A., & Du Laing, G. (2011). Controlled variation of redox conditions in a floodplain soil: impact on metal mobilization and biomethylation of arsenic and antimony. *Geoderma, 160*(3), 414-424.

Gai, X., Wang, H., Liu, J., Zhai, L., Liu, S., Ren, T., & Liu, H. (2014). Effects of feedstock and pyrolysis temperature on biochar adsorption of ammonium and nitrate. *PloS one, 9*(12), e113888.

Hale, S., Alling, V., Martinsen, V., Mulder, J., Breedveld, G., & Cornelissen, G. (2013). The sorption and desorption of phosphate-P, ammonium-N and nitrate-N in cacao shell and corn cob biochars. *Chemosphere, 91*(11), 1612-1619.

Helminen, J., Helenius, J., Paatero, E., & Turunen, I. (2001). Adsorption equilibria of ammonia gas on inorganic and organic sorbents at 298.15 K. *Journal of Chemical & Engineering Data, 46*(2), 391-399.

Hodgson, E., Lewys-James, A., Rao Ravella, S., Thomas-Jones, S., Perkins, W., & Gallagher, J. (2016). Optimisation of slow-pyrolysis process conditions to maximise char yield and heavy metal adsorption of biochar produced from different feedstocks. *Bioresource technology, 214*, 574-581.

Hollister, C. C., Bisogni, J. J., & Lehmann, J. (2013). Ammonium, nitrate, and phosphate sorption to and solute leaching from biochars prepared from corn stover (L.) and oak wood (spp.). *Journal of environmental quality, 42*(1), 137-144.

Hou, J., Huang, L., Yang, Z., Zhao, Y., Deng, C., Chen, Y., & Li, X. (2016). Adsorption of ammonium on biochar prepared from giant reed. *Environmental Science and Pollution Research, 23*(19), 19107-19115.

Jassal, R. S., Johnson, M. S., Molodovskaya, M., Black, T. A., Jollymore, A., & Sveinson, K. (2015). Nitrogen enrichment potential of biochar in relation to pyrolysis temperature and feedstock quality. *Journal of environmental management, 152*, 140-144.

Jeffery, S., Verheijen, F.G.A., van der Velde, M., Bastos, A.C. (2011). A quantitative review of the effects of biochar application to soils on crop productivity using meta-analysis. *Agriculture, Ecosystems & Environment*, 144(1), 175-187.

Komkiene, J., & Baltrenaite, E. (2016). Biochar as adsorbent for removal of heavy metal ions [Cadmium(II), Copper(II), Lead(II), Zinc(II)] from aqueous phase. *International Journal of Environmental Science and Technology, 13*(2), 471-482. doi: 10.1007/s13762-015-0873-3

Mukome, F. N., Zhang, X., Silva, L. C., Six, J., & Parikh, S. J. (2013). Use of chemical and physical characteristics to investigate trends in biochar feedstocks. *Journal of agricultural and food chemistry, 61*(9), 2196-2204.

Mukwaturi, M., & Lin, C. (2015). Mobilization of heavy metals from urban contaminated soils under water inundation conditions. *Journal of Hazardous Materials, 285*, 445-452.

Nartey, O. D., & Zhao, B. (2014). Biochar preparation, characterization, and adsorptive capacity and its effect on bioavailability of contaminants: an overview. *Advances in Materials Science and Engineering, 2014*.

Park, J.-H., Cho, J.-S., Ok, Y. S., Kim, S.-H., Kang, S.-W., Choi, I.-W., Seo, D.-C. (2015). Competitive adsorption and selectivity sequence of heavy metals by chicken bone-derived biochar: Batch and column experiment. *Journal of Environmental Science and Health, Part A, 50*(11), 1194-1204.

Park, J.-H., Ok, Y. S., Kim, S.-H., Cho, J.-S., Heo, J.-S., Delaune, R. D., & Seo, D.-C. (2016). Competitive adsorption of heavy metals onto sesame straw biochar in aqueous solutions. *Chemosphere, 142*, 77-83.

Pellera, F.-M., Giannis, A., Kalderis, D., Anastasiadou, K., Stegmann, R., Wang, J.-Y., & Gidarakos, E. (2012). Adsorption of Cu(II) ions from aqueous solutions on biochars prepared from agricultural by-products. *Journal of environmental management, 96*(1), 35-42. doi:

Reddy, K. R., & DeLaune, R. D. (2008). *Biogeochemistry of wetlands: science and applications*: CRC press.

Schomberg, H. H., Gaskin, J. W., Harris, K., Das, K., Novak, J. M., Busscher, W. J., . . . Ahmedna, M. (2012). Influence of biochar on nitrogen fractions in a coastal plain soil. *Journal of environmental quality, 41*(4), 1087-1095.

Taghizadeh-Toosi, A., Clough, T. J., Sherlock, R. R., & Condron, L. M. (2012). Biochar adsorbed ammonia is bioavailable. *Plant and soil, 350*(1-2), 57-69.

Takaya, C. A., Fletcher, L. A., Singh, S., Anyikude, K. U., & Ross, A. B. (2016). Phosphate and ammonium sorption capacity of biochar and hydrochar from different wastes. *Chemosphere, 145*, 518-527.

Tang, J., Zhu, W., Kookana, R., Katayama, A. (2013). Characteristics of biochar and its application in remediation of contaminated soil. *Journal of Bioscience and Bioengineering,* 116(6), 653-659.

Uzoma, K., Inoue, M., Andry, H., Zahoor, A., & Nishihara, E. (2011). Influence of biochar application on sandy soil hydraulic properties and nutrient retention. *J. Food Agric. Environ, 9*(3-4), 1137-1143.

Van Humbeck, J. F., McDonald, T. M., Jing, X., Wiers, B. M., Zhu, G., & Long, J. R. (2014). Ammonia capture in porous organic polymers densely functionalized with brønsted acid groups. *Journal of the American Chemical Society, 136*(6), 2432-2440.

Wiegand, J., Aschan, G., Kraus, U., Piontek, J., & Mederer, J. (2009). Chemical fractionation and soil-to-plant transfer characteristics of heavy metals in a sludge deposit field of the river Ruhr, Germany. *Soil & Sediment Contamination, 18*(1), 14-29.

Yao, Y., Gao, B., Zhang, M., Inyang, M., & Zimmerman, A. R. (2012). Effect of biochar amendment on sorption and leaching of nitrate, ammonium, and phosphate in a sandy soil. *Chemosphere, 89*(11), 1467-1471.

Zeng, Z., Li, T.-q., Zhao, F.-l., He, Z.-l., Zhao, H.-p., Yang, X.-e., . . . Rafiq, M. T. (2013). Sorption of ammonium and phosphate from aqueous solution by biochar derived from phytoremediation plants. *Journal of Zhejiang University Science B, 14*(12), 1152-1161.

Zhu, K., Fu, H., Zhang, J., Lv, X., Tang, J., & Xu, X. (2012). Studies on removal of NH4+-N from aqueous solution by using the activated carbons derived from rice husk. *Biomass and Bioenergy, 43*, 18-25

Supplementary Materials

1. Supplementary Tables

Table S1 Some major physical and chemical characteristics of the biochar materials and soils used in the experiments

Parameter	SWP550	SWP700	Sandy soil	Contaminated soil
Moisture (%)	1.52	1.00	-	-
Total Carbon (%)	85.5	90.2	-	-
H (%)	2.77	1.83	-	-
O (%)	10.3	6.02	-	-
H:C	0.39	0.24	-	-
O:C	0.09	0.05	-	-
Total Ash (%)	1.25	1.89	-	-
Total N (%)	<0.1	<0.1	-	-
pH	7.91	8.44	9.59	5.98
EC (dS/m)	0.09	0.16	-	-
Total Surface Area (m^2/g)	26.4	162	-	-
PAH (mg/kg)	4.39	0.18	-	-
As (mg/kg)	0.9	0.61	1.92	32.5
Cd (mg/kg)	3.48	8.16	udl	udl
Cr (mg/kg)	34.5	123	udl	2.74
Co (mg/kg)	1.04	4.37	udl	udl
Cu (mg/kg)	19.4	9.66	0.83	172
Pb (mg/kg)	udl	udl	9.64	78.78
Hg (mg/kg)	udl	udl	udl	udl
Mo (mg/kg)	3.36	38.5	udl	udl
Ni (mg/kg)	3.3	74.0	udl	udl
Se (mg/kg)	5.68	udl	udl	udl
Zn (mg/kg)	25.7	99.6	16.4	84.5

udl: under detection limit

Table S2 Details on experimental set-up for Experiment 1

	Biochar (g)	Sandy soil (g)	NH_4Cl dose (mmol/kg)	Water (mL)
Control	0	50	2	10
0.5 g SWP550	0.5	50	2	10
1 g SWP550	1	50	2	10
0.5 g SWP700	0.5	50	2	10
1 g SWP700	1	50	2	10

Table S3 Details on experimental set-up for Experiment 2

	Soil (g)	Grass clippings (g)	Biochar (g)	Water (mL)
Control	50	5	0	150
0.5 g SWP550	50	5	0.5	150
1 g SWP550	50	5	2	150
0.5 g SWP700	50	5	0.5	150
1 g SWP700	50	5	2	150

2. Supplementary Figure

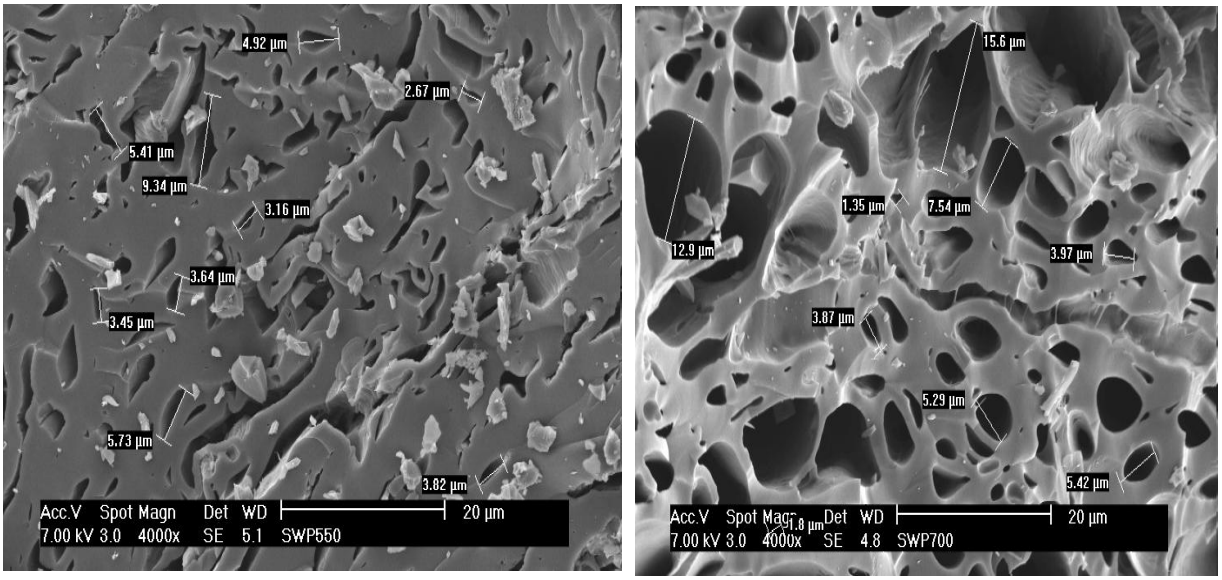

Figure S1 SEM images of SWP550 (a) and SWP700 (b). Scanning electron micrographs of SWP550 and SWP700 showed observable differences as pyrolysis temperature of the biochar material increased. For both images, a porous surface was revealed with thicker pore walls for SWP550 (left) and thinner pore walls for SWP700 (right) with a greater number of pores visible for

SWP700, indicating a high surface area that SWP550. The larger surface area of SWP700 may be more favourable for nitrogen retention and for trace element immobilization.